A Study on the Nucleation and Evolution of Hydrogen Induced Cracking in Pipeline Steel

Lazcano-Ugalde E. M, González-Velázquez J.L.*, Morales-Ramírez A. de J.

Instituto Politécnico Nacional, ESIQIE, Unidad Profesional Adolfo López Mateos, Edificio 8, Zacatenco, C.P. 07300 México D.F jlgonzalez@ipn.mx

ABSTRACT. A metallographic and fractographic study by scanning electron microscopy study of the nucleation and evolution of hydrogen induced cracking (HIC) growth was done. The HIC cracks were induced by cathodic charging and its growth was monitored by straight beam ultrasonic mapping, so the nucleation sites as well as the cracking evolution could be identified and measured. The results showed that there are inclusions that nucleate HIC in very short times and others nucleate cracks only after hundreds of hours after hydrogen charging, but the early nucleation sites are usually clusters of inclusions, rather than individual ones. It was observed that the HIC growth is composed of two mechanisms: the growth of individual cracks and the interconnection of several cracks to form larger cracks that continue growing themselves and by interconnecting with other cracks. The interconnection mechanism can be by direct interconnection of coplanar cracks or by out of plane interconnection, where crack deflection plays a very important role. The study is completed with observations of the crack path and the kinetics of HIC growth for both, overall and individual HIC.

INTRODUCTION

Hydrogen Induced Cracking (HIC) is a common problem in the oil and natural gas industry, especially in the transport of hydrocarbons with high H_2S and CO_2 contents known as sour [1, 2]. Generally, the HIC process can be considered as a nucleation and growth phenomenon which consists in the progressive accumulation of molecular hydrogen in trapping sites that serve as crack nuclei. The hydrogen is a product of the corrosion process between the steel pipe and the sour environment, which diffuses into the pipe wall and it turns into a molecular gas in certain trapping sites, developing high pressures that form a cavity which is the HIC indeed [3,4]. As the hydrogen continues accumulating in the cavity, an internal crack is formed and it grows to become a macroscopic crack.

It is generally accepted that the MnS inclusion size and shape controls the nucleation of the HIC; specifically large and elongated MnS inclusions are considered the preferred nucleation sites for HIC, so the basis for developing sour environment

resistant steels is to control the MnS inclusion content by drastically reducing the S content and controlling the shape of the inclusions by calcium and rare earth additions. Even though this strategy has proven to produce steel with greater resistance to HIC, nowadays it is not completely understood how the nucleation and growth of HIC takes place, specifically why the cracks initiate at preferential sites, as well as how this affects the rate of crack propagation once the process has begun. Gyu Tae Park [5] and Xuechong Ren [6] have demonstrated that the steel microstructure and not only the inclusion content, plays a key role in the nucleation on the HIC, by showing that the ferrite alone is particularly susceptible to the HIC cracking because it easily absorbs hydrogen, so something else, in addition to the MnS inclusion size and shape should influence the nucleation and growth of HIC in low carbon steels.The aim of this work is to investigate the characteristics of the nucleation sites during the HIC process, as well as to observe the evolution and kinetics of HIC.

EXPERIMENTAL PROCEDURE

Plates of pipeline steel were exposed to cathodic hydrogen charging in order to produce the HIC in controlled conditions. The plates were 12 cm (4.72 in) wide and 18 cm (7.09 in) long and were machined to get parallel faces. The plates were extracted form pipes of different thickness: 1.27 cm (0.5 in) for the plates designated as A and 1.77 cm (0.7 in) in the B plates. The chemical composition and the mechanical properties of both plates are shown in Table I, whereas the microstructural properties are given in Table II. The plate surfaces were ground with silicon carbide paper up to the 600 grade and then were inspected with an ultrasonic flaw detector using a straight beam transducer of 20 MHz frequency and 0.5 cm (0.2 in) diameter in order to verify the absence of internal cracks and defects. Then, the plates were cleaned by immersion in an ultrasonic bath for 10 min using a commercial cleaning solution. Once the plates were dry and clean, an acrylic cell was glued to one face of the plate and the cell was filled with the electrolytic solution.

In order to generate hydrogen, the steel plate is connected as a cathode to an external DC power supply and a platinum bar is connected as anode; the applied current density was 2.48 mA cm^{-2}. The electrolyte solution is sulphuric acid in bidistilled water at0.4 wt. %,"charged" with 5 drops of a "poison solution", consisting of 4 g of phospurous (99.5%) disspersed in 100 mL of CS_2 (Aldrich, 99%) which promotes the absortion of hydrogen into the plate. Once the the system is turned on, the electrolyte solution was renewed every 3 days and five drops of the "poison solution" were added daily, all of this in order to enssure the uniformity of the hydrogen charge. The experimental setup is shown in Figure 1.

The HIC growth was monitored by mapping the face of the plate oposite to the face exposed to the electrolyte solution, marking with permanent ink marker the contours of the HIC cracks. Once most of the area of the plate exposed to cathodic charging was

cracked, the cathodic charging was discontinued and the plates were cut to open the cracked areas selected for fractographic examination.

Table 1. Chemical composition and mechanichal properties of steel plates tested.

Element	C	Si	Mn	P	S
Plate A	0.061	0.210	0.845	0.024	0.014
Plate B	0.067	0.275	1.093	0.016	0.011

HRB	E / Mpa	V	YS / Mpa	UTS / Mpa	Elongation / %	CV / J
86-90	207000	0.3	360	540	16	68

Table II. Microestructural properties of the steel plates tested.

Plate	Inclusions / %V	Longitudinal		Transversal	
		% Ferrite	%Perlite	% Ferrite	% Perlite
A	0.071	92.72	7.28	87.97	12.02
B	0.091	94.94	5.06	94.31	5.69
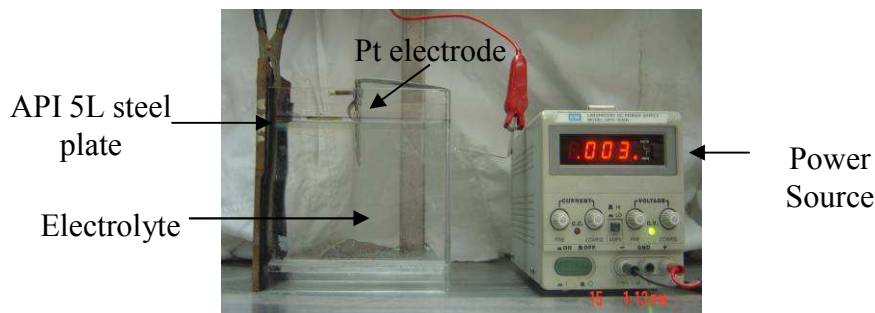
Figure 1. Experimenal setup for cathodic charging.

RESULTS AND DISCUSSION

The ultrasonic mapping of Plate A during hydrogen cathodic charging is shown in Figure 2. It is observed that the first HIC cracks are detected after 2 days of cathodic charging. In the first 4 days, the cracks formed grew preferentially in the longitudinal direction. After 10 days, the first cracks were still growing, but the growth was more important in the transversal direction, whereas new cracks begun to grow in the same way as the early nucleated cracks. It is important to point that in this stage, some cracks that were close to each other started to interconnect, as it can be observed in the B4 zone of the mapping shown in figure 2. Finally, between the 13th and 28th days of hydrogen charging, the nucleation of new cracks stopped and the cracks formed in the previous days continued growing mainly by interconnection with the sorrounding cracks.
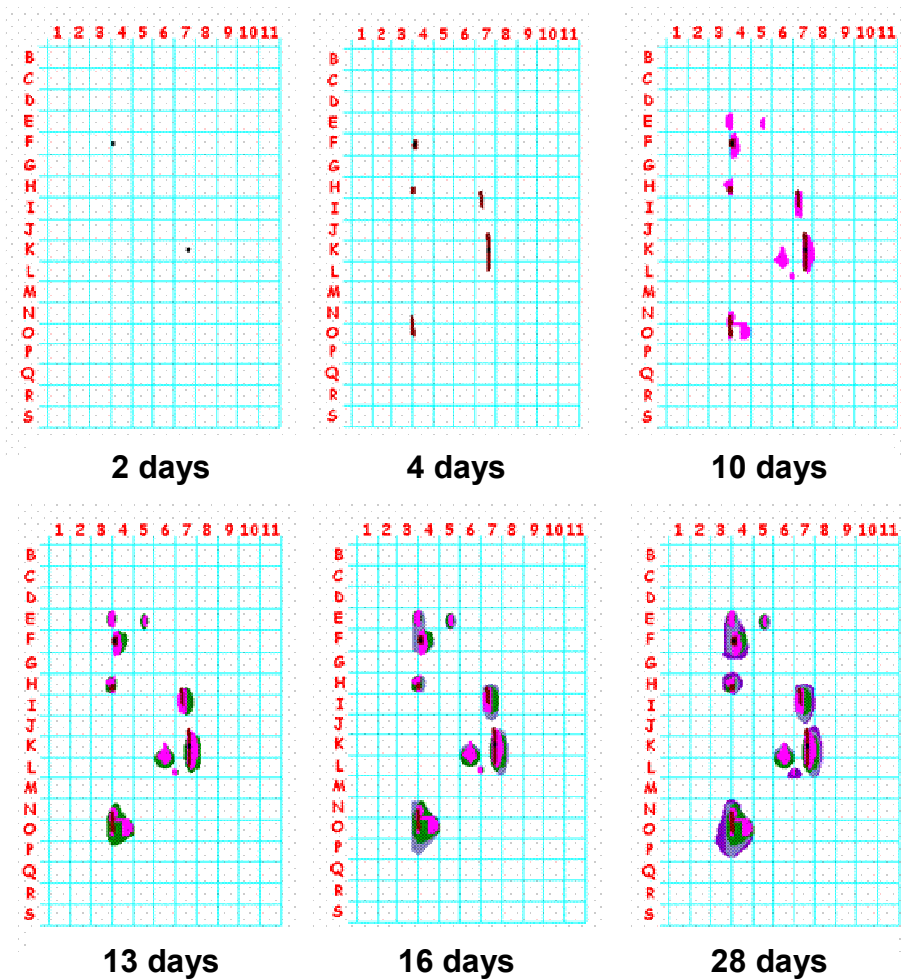
Figure 2. Crack contours by ultrasonic mapping of Plate A.

The ultrasonic mapping for Plate B is shown in Figure 3. In this case, the first cracks also nucleated after 2 days of cathodic charging, however, the number of nucleated cracks was 12, while in in the Plate A there were only 2 cracks after 2 days.The first nucleated cracks began their growth at a nearly linear rate, but after 8 days, their growth rate decreaced. After 15 days, the cracks started to interconnect, as can be seen in the H6 zone of the mapping shown in figure 3. Finally, between the 15th and 35th days, there is no formation of new cracks, and the already formed ones continued their growth by interconnection with other cracks and the growth rate decreased drastically.

The HIC cracked area growth as a function of time is for plates A and B is shown in the Figure 4. As can be seen, both plates present the same behavior: in the early stages of cathodic charging, up to 400 hours of hydrogen charging, the cracks grew at rates of 2.93 and 2.94 mm^{2}h^{-1} rate for plates A and B respectively and the HIC consisted basically of the growth of individual cracks. After this initial stage, the growth rate did

reduce drastically to be almost constant after 800 hrs of hydrogen charging. In the second stage, the HIC growth in both series of plates was by the interconnection of cracks. It is important to point out that, independently of the number of nucleated cracks (which was much higher in Plate B than in plate A), the final cracked area for both plates was almost the same after 800 hrs; this result may indicate that the HIC kinetics is controlled by the growth process and not by the nucleation.
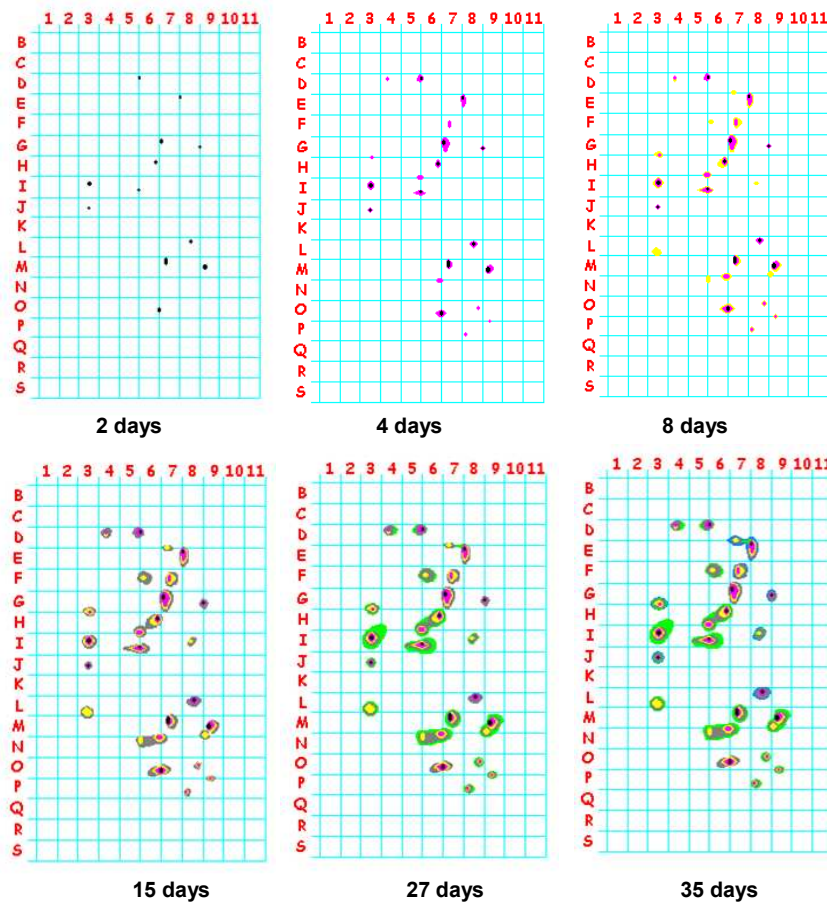
Figure 3. Crack contours by ultrasonic mapping of Plate B.
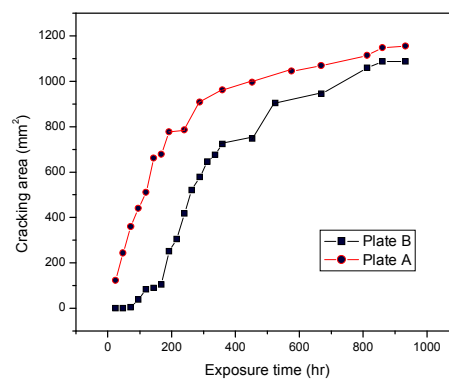
Figure 4. Crack growth rate for Plates A and B.

The growth rates for individual cracks for both Plates A and B is shown in Figure 5. These individual cracks were those with no interconnection events, so its individual behavior could be observed. As can be seen in figure 5, the individual cracks in both plates had the same behavior of the overall rates, with an initially rapid growth rate up to 400 hrs, and reducing the growth rate after 800 hrs.
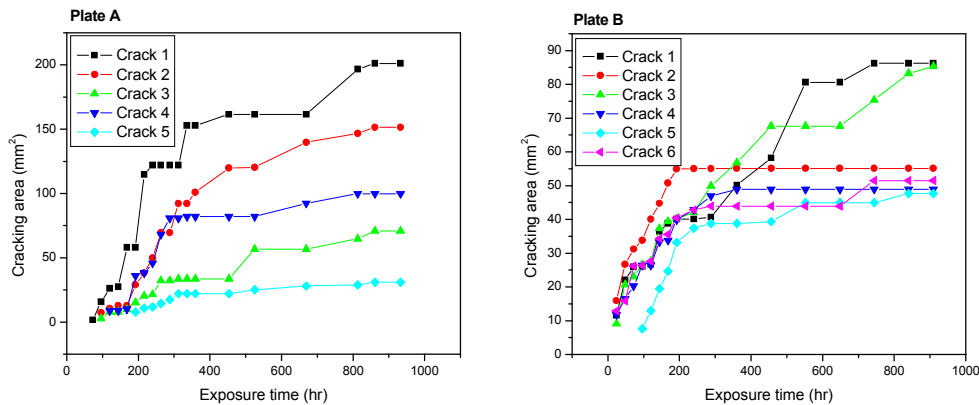
Figure 5. Individual growth rates for individual cracks, a) Plate A, b) Plate B

The crack path through the microstructure was observed by a metallographic preparation of the thickness section of the cracked plates and microscopic observation focused to cracks formed in short times, referred as early cracks and those formed after approximately 400 hrs of cathodic charging. The examination of the cracked plates, of which an example is shown in Figure 6, confirmed that the mechanism of HIC growth can be: the growth of individual cracks that do not interconnect and the growth by interconnection of individual craks. The growth of individual cracks can be explained by the widely accepted pressure model, but the interconnection of cracks is more complex. As seen in figure 6, there are three different mechanisms of interconnection: Direct interconnection of two cracks that are in the same plane (Zone 2), interconnection of craks in different planes by crack deflection (Zone 3), and finally, the interconnection of out of plane cracks by secondary cracking (Zone 4).

The figure 7 shows the fracture surface observed by SEM of an early formed HIC crack in the Plate A. As can be observed, the early HIC nucleated in areas with clusters of MnS inclusions, while other inclusions that were even larger nucleated cracks after a long time of hydrogen charging or did not nucleate cracks at all, as seen in figure 7b. The chemical composition of the inclusions that served as nuclei was confirmed by EDS analysis. The fracture surface is characterized by the unbroken MnS inclusions and a cuasi-cleavage fracture of the ferrite and pearlite colonies that surround the inclusions. No difference of the fracture surface features is observed between the areas near the crack nuclei and the propagation areas away of them. The fact that the inclusion clusters serve as HIC nuclei, rather than the large and elongated individual inclusions indicate that the matrix-inclusion inerface areas are the hydrogen traps. So, since the clusters have a higher interface area than individual inclusions of size even larger than the length of the cluster, they are more likely to be a HIC nucleous.
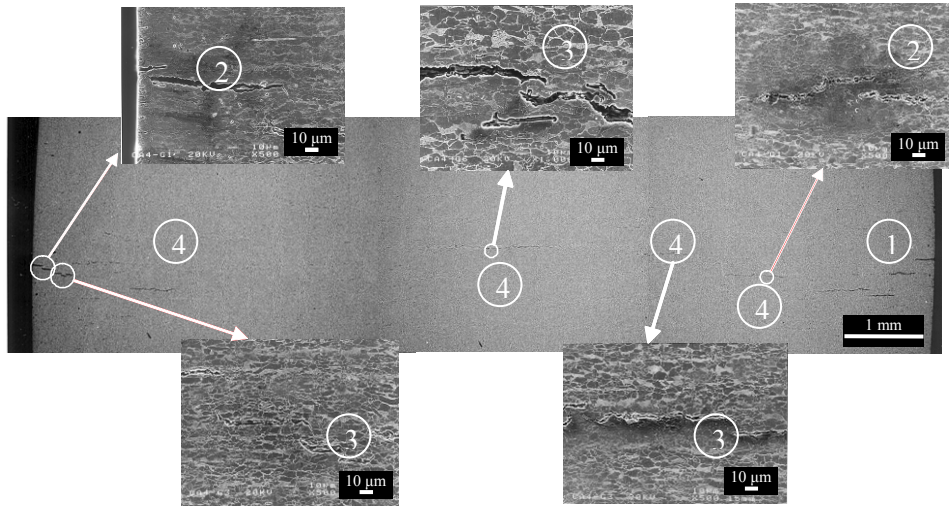
Figure 6. HIC propagation path through the microstructure.
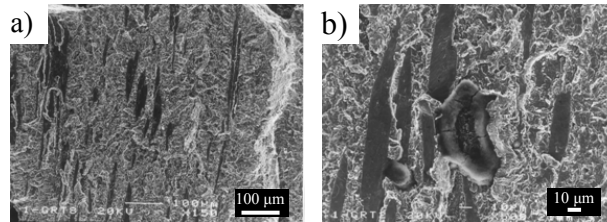
Figure 7. a) Fracture surface of an early nucleation HIC in Plate A. b) Large MnS inclusion in the propagation zone.

The Figure 8 shows an early nucleation sites for HIC in plate B, it can be observed that the area has clusters of MnS inclusions, while far from the nucleous there were not nucleated cracks. One cracked area of the Plate B was opened to observe the fracture surface as shown in Figure 9. This crack was a late one that originated after 192 hrs of hydrogen charging. As can be observed, this site has a large and isolated MnS inclusion.
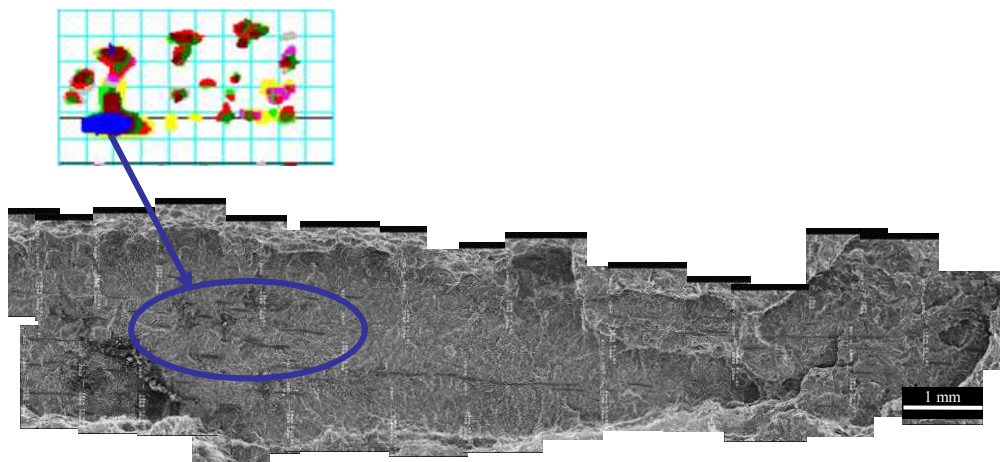
Figure 8. Cluster of MnS inclusions which is an early nucleation site of HIC.
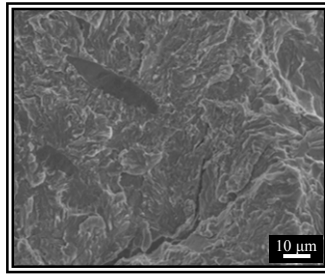
Figure 9. Fracture surface of a late HIC nucleation site in Plate B.

CONCLUSIONS

The kinetics of HIC growth in API 5L steel plates was measured by ultrasonic mapping of the cracked area as the HIC was induced by hydrogen cathodic charging, the cracking process began with the nucleation and growth of individual cracks, which nucleate in clusters of MnS inclusions. The individual cracks grew by the classic pressure mechanism and then by interconnection by three different mechanisms: direct interconnection of cracks in the same plane, interconnection of cracks in different planes by crack deflection and out of plane interconnection by secondary cracking.

The growth rate was in two stages: the initial one which is characterized by a relatively high crack growth rate and the growth of individual cracks, this behavior was observed up to 400 hrs of hydrogen charging, and the late one characterized by slower growth rates and growth by the interconnection of cracks.

REFERENCES

1. Dey S., Mandhyan A.K., Sondhi S.K., Chattoraj I. (2006) *Corrosion Science* **48** 2676-2778
2. J. L. González, R. Ramírez, J. M. Hallen y R. A. Guzman. (1997) *Corrosion* **53** 935-943
3. Taira T., Kobayashi Y., Matsumoto K., Tsukada K. (1984) *Corrosion-NACE* **40 5-16**
4. Hara T., Asahi H., Ogawa H, (2004) *Corrosion Science* **60** *325-329*
5. Tae P. G., Koh S. U., Jung H. G., (2008) **50** 1865-1871
6. Ren X., Chu W., Li J., Su Y., Qiao L. (2008) *Mat. Chem, Phys.* **107** 231-235